Stationary equilibrium of test particles near charged black branes with the hyperscaling violating factor

Yu-Qi Lei and Xian-Hui Ge*

Department of Physics, Shanghai University, 99 Shangda Road, Shanghai 200444, China

We explore the upper bound of the Lyapunov exponent for test particles that maintain equilibrium in the radial direction near the charged black brane with the hyperscaling violating factor. The influences of black brane parameters (hyperscaling violation exponent θ and dynamical exponent z) are investigated. We show that the equilibrium in the radial direction of test particles can violate the chaos bound. The chaos bound is more easily violated for the near-extremal charged black branes. When the null energy condition ($T_{\mu\nu}\xi^{\mu}\xi^{\nu} \geq 0$) is broken, the bound is also more likely to be violated. These results indicate that the chaos bound of particle motion is related to the temperature of the black hole and the null energy condition (NEC). By considering the zero-temperature and $T_{\mu\nu}\xi^{\mu}\xi^{\nu} = 0$ cases, we obtain the critical parameters θ_c and z_c for the violation of chaos bound. The chaos bound is always satisfied in the range $\theta > \theta_c$ or $z > z_c$.

I. INTRODUCTION

Chaos is an important nonlinear phenomenon that describes the sensitive response of the evolution of a system to the initial conditions. To illustrate the strength of chaotic phenomena, the Lyapunov exponent can be introduced. When a chaotic system is perturbed, the perturbation grows exponentially with time, and its corresponding exponent is the Lyapunov exponent. The larger the Lyapunov exponent, the more chaotic the test particle. As black hole theory is a kind of nonlinear theory, it is normal to see chaos in studying black holes. Chaos often exists in various objects, for example, the chaotic trajectories near black holes [1–9] and the chaos in black hole thermodynamics [10–14]. The nature of black hole chaos needs to be further explored.

Maldacena, Shenker, and Stanford derived a universal temperature-dependent upper bound of the Lyapunov exponent λ in quantum chaotic systems by the quantum field theory [15]

$$\lambda \leq \frac{2\pi T}{\hbar}, \qquad (1)$$

where T is the temperature of the system. Such temperature-dependent characteristics can also be obtained

*Corresponding author.
gexh@shu.edu.cn

through the thought experiment of the shock wave near the horizon of a black hole [16,17], and some calculations of the shock wave have studied the Lyapunov exponent near the horizon [18–20]. In black hole calculations, the equivalent form of the chaos bound can be obtained by the natural unit $\hbar = 1$ and the relationship between the Hawking temperature T_H at the black hole's event horizon and the surface gravity κ

$$\lambda \leq \kappa. \qquad (2)$$

In the background of black holes, this upper bound can be tested in single-particle systems. Hashimoto and Tanahashi obtained a consistent upper bound of the Lyapunov exponent by considering the test particles maintain the static equilibrium due to external forces outside the black hole [21]. This result inspires the study of the Lyapunov exponent's upper bound outside black holes by considering particle motion.

In [22], Zhao *et al.* studied the static equilibrium of charged particles near a large class of charged black holes and discussed the near-horizon expansion. They found that in the static equilibrium of the test particle, the bound Eq. (2) is satisfied by Reissner-Nordström (RN) and Reissner-Nordström anti–de Sitter (RN-AdS) black holes and can be violated by some black holes [22]. The violation of the upper bound for the Lyapunov exponent was also found in the black hole with quasitopological electromagnetism [23]. Taking into account the effects of angular momentum, the circular motion of the test particle can violate the chaos bound for the RN black hole [24], the Kerr-Newman black hole [25] and the Kerr-Newman AdS black hole [26]. Different black holes were discussed to

investigate the violation of chaos bound [27–32]. In [33], the Lyapunov exponent of particle motion near the black hole and cosmological horizons was investigated, and the author pointed out that the null energy conditions do not guarantee the satisfaction of chaos bounds. One of the interesting questions is what properties of black holes are associated with the Lyapunov exponent, which inspires us to study the Lyapunov exponent of particle motion.

In this paper, we investigate the relationship between the Lyapunov exponent and the chaos bound when the test particle maintains a stationary equilibrium in the radial direction near the charged black brane. We focus on the equilibrium in the radial direction of test particles. The charged black brane has the hyperscaling violating factor [34]. The hyperscaling violating factor can bring interesting properties to space-time geometry. Other several hyperscaling violating black brane solutions were proposed [35–38]. The influence of the lateral momentum is considered to explore the bound violation. Charged particles can maintain an equilibrium in the radial direction near the horizon by the repulsive force from the electric charge and the lateral momentum. We do not consider the backaction of particle motion on the background spacetime. The influence of the two characteristic parameters of the charged black brane, the dynamical exponent z and the hyperscaling violating exponent θ, on the Lyapunov exponent is discussed. We found that the chaos bound can be violated in the parameter range where θ and z are small. In our previous work [24], it was pointed out that the chaos bound can be violated in the case of near-extremal charged black holes, so here we discuss the effect of the temperature of the charged black brane on the Lyapunov exponent of particle motion. We also consider the effect of the null energy condition (NEC) on the study of the chaos, and the expression of NEC is $T_{\mu\nu}\xi^{\mu}\xi^{\nu} \geq 0$. Our numerical results show that the bound can be violated when the NEC is violated. In the extremal cases of zero-temperature and satisfying NEC, we derive the critical parameters θ_c and z_c, and find the chaos bound $\lambda \leq \kappa$ is satisfied when $\theta > \theta_c$ or $z > z_c$.

The rest of this paper is organized as follows. In Sec. II, we review the background of the charged black branes with the hyperscaling violating factor and its parameter relationship of the temperature and NEC. In Sec. III, we derive the Lyapunov exponent λ for test particles that maintain equilibrium in the radial direction using the Jacobian matrix. In Sec. IV, the numerical results of $\kappa^2 - \lambda^2$ are shown. We discuss the influences of temperature T_H, parameters (θ and z) and the null energy condition to the Lyapunov exponent. The violation of the chaos bound is found. In Sec. V, the critical parameters θ_c and z_c are obtained from the extremal cases of black brane temperature and satisfying NEC. We summarize the main conclusions in Sec. VI. In the Appendix, we discuss the case of the black brane with the violation of NEC.

II. REVIEW OF THE CHARGED BLACK BRANES WITH THE HYPERSCALING VIOLATING FACTOR

The charged black brane with the hyperscaling violating factor considered is a solution to the Einstein-Maxwell-dilaton theory. The Einstein-Maxwell-dilaton gravity has a $d + 2$-dimensional minimal model with action [34,35,38]

$$S = -\frac{1}{16\pi G} \int d^{d+2}x\sqrt{-g}$$
$$\times \left[R - \frac{1}{2}(\partial\phi)^2 + V(\phi) - \frac{1}{4}\sum_{i=1}^{2} e^{\lambda_i\phi}F_i^2 \right], \quad (3)$$

where R is the Ricci scalar, ϕ is the scalar field and $V(\phi)$ is the potential function of scalar field. The model has two free parameters λ_1, λ_2 and two gauge fields F_1, F_2.

The charged black brane solution with hyperscaling violating factor from the action Eq. (3) can be written as [34]

$$ds^2 = r^{-2\frac{\theta}{d}}\left(-r^{2z}f(r)dt^2 + \frac{dr^2}{r^2 f(r)} + r^2 d\vec{x}^2 \right),$$
$$F_{1\,rt} = \sqrt{2(z-1)(z+d-\theta)}e^{\frac{\theta(1-d)/d+d}{\sqrt{2(d-\theta)(z-1-\theta/d)}}\phi_0}r^{d+z-\theta-1},$$
$$F_{2\,rt} = Q\sqrt{2(d-\theta)(z-\theta+d-2)}e^{-\sqrt{\frac{z-1-\theta/d}{2(d-\theta)}}\phi_0}r^{-(z+d-\theta-1)},$$
$$e^{\phi} = e^{\phi_0}r^{\sqrt{2(d-\theta)(z-1-\theta/d)}}, \quad (4)$$

where ϕ_0 is a constant scalar field. The parameters z and θ are the dynamical and hyperscaling violating exponents, respectively, with $z > 1$ and $0 \leq \theta < d$. It should be noted that this solution will not be valid when $\theta = d$. The blacken factor $f(r)$ is given by

$$f(r) = 1 - \frac{M}{r^{z+d-\theta}} + \frac{Q^2}{r^{2(z+d-\theta-1)}}, \quad (5)$$

where M is the mass of black brane and Q is the electric charge. $F_{1\,rt}$ is an auxiliary gauge field and $F_{2\,rt}$ is the electric field. Taking infinity as the reference point of the electric potential, the electric potential function A_t is given by

$$A_t = \int_{\infty}^{r} F_{2\,rt}dr = -\frac{\sqrt{2}Qe^{-\phi_0\sqrt{\frac{d-dz+\theta}{2d(d-\theta)}}}r^{2-d-z+\theta}}{\sqrt{d+z-\theta-2}} \quad (6)$$

The constraint $d + z - \theta - 2 \geq 0$ can ensure that the electric potential function is real. The radius of horizon r_h can be defined by $f(r_h) = 0$, which can lead to

$$r_h^{2(d+z-\theta-1)} - Mr_h^{d+z-\theta-2} + Q^2 = 0. \quad (7)$$

The Hawking temperature T_H at the horizon is given by

$$T_H = \frac{(d+z-\theta)r_h^z}{4\pi}\left(1 - \frac{(d+z-\theta-2)Q^2}{d+z-\theta}r_h^{2(\theta-d-z+1)} \right). \quad (8)$$

We can obtain the corresponding surface gravity κ, that is to say

$$\kappa = 2\pi T_H = \frac{(d+z-\theta)r_h^z}{2}$$
$$\times \left(1 - \frac{(d+z-\theta-2)Q^2}{d+z-\theta} r_h^{2(\theta-d-z+1)} \right). \quad (9)$$

To avoid naked singularity, the following inequality must be satisfied

$$r_h^{2(d+z-\theta-1)} \geq \frac{(d+z-\theta-2)}{d+z-\theta} Q^2. \quad (10)$$

With the null vector $\xi^\mu = (\sqrt{g^{rr}}, \sqrt{g^{tt}}, 0)$, the null energy condition (NEC) of the black brane Eq. (4) is [34]

$$T_{\mu\nu}\xi^\mu\xi^\nu \sim d(\alpha+1)(\alpha+z-1)r^{-2\alpha}f(r) \geq 0, \quad (11)$$

where $\alpha = -\frac{\theta}{d}$. The NEC can be recast as

$$(\alpha+1)(\alpha+z-1) \geq 0. \quad (12)$$

Here we can obtain all the parameter conditions satisfied by the charged black brane with the hyperscaling violating factor

$$d+z-\theta-2 \geq 0,$$
$$r_h^{2(d+z-\theta-1)} \geq \frac{(d+z-\theta-2)}{d+z-\theta} Q^2, (\alpha+1)(\alpha+z-1) \geq 0. \quad (13)$$

Among the parametric constraints, the null energy condition (NEC) is an important element, and it is one of the key parts of our discussion. Since the violation of NEC is controversial, we put the case of the spacetime with the violation of NEC in the appendix as a referenceable supplementary discussion. In such background, the null energy condition $T_{\mu\nu}\xi^\mu\xi^\nu \geq 0$ is violated.

We focus on the effect of the hyperscaling violating exponent θ and the dynamical exponent z, so to simplify the calculation we set the parameters

$$\phi_0 = 0 \quad \text{and} \quad r_h = 1. \quad (14)$$

The inequality Eq. (10) can be recast as

$$1 \geq \frac{(d+z-\theta-2)}{d+z-\theta} Q^2, \quad (15)$$

and there is no extremal black brane when $Q^2 < 1$. In the study of RN black holes, we pointed out the violation of chaos bound in the near-extremal RN black hole [24]. Thus it is interesting to discuss the Lyapunov exponent of
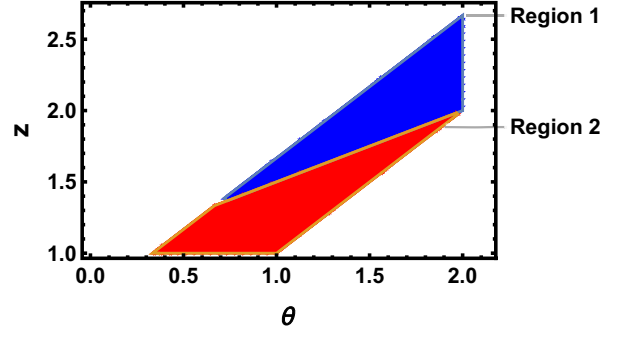

FIG. 1. The available physical space (θ, z), when $d = 2$, $\phi_0 = 0$, $Q = 2$ and $r_h = 1$. Region 1 describes the charged black brane with hyperscaling violating factor. Region 2 corresponds to the case where the null energy condition is violated.

particle motion in the extremal and near-extremal charged black brane. To explore the cases of extremal and near-extremal black brane and present results more clearly, we consider the charge of the black brane $Q = 2$ in this paper.

In this work, we focus on the 4-dimensional cases, and we set the dimensional parameter $d = 2$. The physical parameter space (θ, z) describing the charged black branes and the spacetime with the violation of NEC is plotted in Fig. 1. As shown in the plot, Region 1 in blue represents the charged black brane with the hyperscaling violating factor. The red region 2 indicates the background where NEC is violated, which is discussed in the appendix. In the parameter space (θ, z), the bottom of charged black branes (Region 1) means $T_{\mu\nu}\xi^\mu\xi^\nu = 0$, and under this boundary, NEC is broken.

III. THE LYAPUNOV EXPONENT OF CHARGED PARTICLES WITH EQUILIBRIUM IN THE RADIAL DIRECTION

We focus on the equilibrium in the radial direction of test particles near the horizon, which means its radial position is a constant. Near a black hole, the equilibrium in the radial direction can be represented as the circular motion of test particles on the equatorial plane of the black hole. Static equilibrium is a special case of the equilibrium in the radial direction that indicates that test particles remain stationary in space. Near the horizon, when a particle in equilibrium is perturbed, its perturbation grows exponentially with time, and its corresponding exponent is the Lyapunov exponent [21]. From the effective potential analysis, this instability of the test particles' equilibrium in the radial direction corresponds to a local maximum of the effective potential of test particles. More discussion of the effective potential about particle motion near horizon can be found in [25–27].

The Lyapunov exponent of test particle also can be calculated by using the Jacobian matrix [39–41]. Here we calculate the Lyapunov exponent of test particles that maintain an equilibrium in the radial direction near the

charged black brane. For simplicity, we rewrite the black brane's metric Eq. (4) as

$$ds^2 = -F(r)dt^2 + \frac{dr^2}{H(r)} + G(r)d\vec{x}^2, \qquad (16)$$

where $F(r) = r^{2(z-\frac{\theta}{d})}f(r)$, $H(r) = r^{2(1+\frac{\theta}{d})}f(r)$, and $G(r) = r^{2(1-\frac{\theta}{d})}$. When we focus on the 4-dimensional case, which can result in $d = 2$ and $d\vec{x}^2 = dx^2 + dy^2$. Consider a charged particle moving in the $y = 0$ plane, its Lagrangian can be written

$$\mathcal{L} = \frac{1}{2}\left(-F(r)\dot{t}^2 + \frac{\dot{r}^2}{H(r)} + G(r)\dot{x}^2\right) - qA_t(r)\dot{t}, \quad (17)$$

where the dot denotes a derivative with respect to the proper time τ. The generalized momenta $\pi_\mu = \frac{\partial \mathcal{L}}{\partial \dot{x}^\mu}$ are

$$\pi_t = -(F(r)\dot{t} + qA_t(r)) = -E = \text{Constant},$$

$$\pi_r = \frac{\dot{r}}{H(r)},$$

$$\pi_x = G(r)\dot{x} = \text{Constant}, \qquad (18)$$

where E is the energy of the test particle, π_r is the radial momentum and π_x is the lateral momentum. The different values of constants (q, π_t, π_x) of test particles result in different states of particle motion, such as falling into the horizon, moving away from the horizon, periodic motion, and stationary equilibrium, etc.

With the formula $\mathcal{H} = \pi_\mu \dot{x}^\mu - \mathcal{L}$, the Hamiltonian of the test particle is

$$\mathcal{H} = \frac{1}{2}\left(-\frac{(\pi_t + qA_t(r))^2}{F(r)} + H(r)\pi_r^2 + \frac{\pi_x^2}{G(r)}\right), \quad (19)$$

which leads to the canonical equations of motion for the test particle

$$\dot{x}^\mu = \frac{\partial \mathcal{H}}{\partial \pi_\mu}, \qquad \dot{\pi}_\mu = -\frac{\partial \mathcal{H}}{\partial x^\mu}. \qquad (20)$$

The radial evolution equations of the test particle with respect to the coordinate time t are

$$\frac{dr}{dt} = \frac{\dot{r}}{\dot{t}} = -\frac{\pi_r F(r)H(r)}{\pi_t + qA_t(r)},$$

$$\frac{d\pi_r}{dt} = \frac{\dot{\pi}_r}{\dot{t}} = \frac{1}{2}\left(\frac{(\pi_t + qA_t(r))F(r)'}{F(r)}\right.$$
$$\left. + \frac{F(r)(H(r)'G(r)^2\pi_r^2 - G(r)'\pi_x^2)}{(\pi_t + qA_t(r))G(r)^2} - 2qA_t(r)'\right), \quad (21)$$

where the prime "$\prime$" denotes derivative with respect to r. We can consider the four-velocity normalization condition

$$g_{\mu\nu}\dot{x}^\mu \dot{x}^\nu = \eta, \qquad (22)$$

where η is the normalization constant with $\eta = -1$ the timelike orbits, $\eta = 0$ the null orbits, and $\eta = 1$ the spacelike orbits. Here, we consider the charged test particle moving along the timelike orbits and the null orbits.

We can obtain the Jacobian matrix of test particle motion by taking (r, π_r) as the phase space variables. For the convenience of writing, we will mark the equations (21) as $\frac{dr}{dt} = M_1$ and $\frac{d\pi_r}{dt} = M_2$. The Jacobian matrix K_{ij} can be defined by

$$K_{ij} = \begin{pmatrix} \frac{\partial M_1}{\partial r} & \frac{\partial M_1}{\partial \pi_r} \\ \frac{\partial M_2}{\partial r} & \frac{\partial M_2}{\partial \pi_r} \end{pmatrix}. \qquad (23)$$

For the equilibrium in the radial direction of test particles, it should satisfy the equilibrium condition $\frac{dr}{dt} = \frac{d\pi_r}{dt} = 0$. The Jacobian matrix K_{ij} of test particles can be reduced at the equilibrium position $r = r_0$. The components are

$$K_{11} = 0,$$

$$K_{12} = -\left.\frac{F(r)H(r)}{\pi_t + qA_t(r)}\right|_{r=r_0},$$

$$K_{21} = -\frac{1}{2}\left(2qA_t(r)'' - \left(\frac{(\pi_t + qA_t(r))F(r)'}{F(r)}\right)'\right.$$
$$\left. + \left(\frac{\pi_x^2 F(r)G(r)'}{(\pi_t + qA_t(r))G(r)^2}\right)'\right)\bigg|_{r=r_0},$$

$$K_{22} = 0. \qquad (24)$$

The eigenvalues of the Jacobian matrix K_{ij} can lead to the Lyapunov exponent λ at the equilibrium position $r = r_0$

$$\lambda^2 = \frac{F(r)H(r)}{2(\pi_t + qA_t(r))}\left(2qA_t(r)'' - \left(\frac{(\pi_t + qA_t(r))F(r)'}{F(r)}\right)'\right.$$
$$\left. + \left(\frac{\pi_x^2 F(r)G(r)'}{(\pi_t + qA_t(r))G(r)^2}\right)'\right)\bigg|_{r=r_0}. \qquad (25)$$

We discuss the effect of the lateral momentum π_x on the particle motion, and the relationship between the constants q, π_t and π_x in the above equation is contracted by the equilibrium condition $\frac{dr}{dt} = \frac{d\pi_r}{dt} = 0$. We can see that the test particle at the equilibrium position $r = r_0$ satisfies

$$\pi_t = \left. \frac{G(r)(\eta G(r) - \pi_x^2)(2F(r)A_t(r)' - A_t(r)F(r)') - \pi_x^2 A_t(r)F(r)G(r)'}{2G(r)A_t(r)'\sqrt{F(r)G(r)(\pi_x^2 - \eta G(r))}} \right|_{r=r_0},$$

$$q = \left. \frac{G(r)F(r)'(\eta G(r) - \pi_x^2) + \pi_x^2 F(r)G(r)'}{2G(r)A_t(r)'\sqrt{F(r)G(r)(\pi_x^2 - \eta G(r))}} \right|_{r=r_0}. \tag{26}$$

Taking the values of π_t and q obtained from the above equations into Eq. (25), we can analyze the effect of π_x in the Lyapunov exponent. The normalization constant $\eta = -1, 0$ corresponds to the timelike orbits and the null orbits, respectively. We label the Lyapunov exponent as λ_s when the particle maintains a static equilibrium (the lateral momentum $\pi_x = 0$), the Lyapunov exponent for timelike orbits as λ_t, and the Lyapunov exponent for null orbits as λ_n. From Eqs. (25) and (26), we can obtain $\lim_{\pi_x \to \infty} \lambda_t = \lambda_n$, which means the Lyapunov exponent of timelike orbits is equal to that of the null orbit when $\pi_x \to \infty$. So when we want to discuss the Lyapunov exponent of massive particles in the limit that $\pi_x \to \infty$, we can consider λ_n of null orbit.

IV. THE ANALYSIS OF THE LYAPUNOV EXPONENT NEAR CHARGED BLACK BRANES

In this section, we discuss the relationship between the chaos bound and the Lyapunov exponent for charged particles which maintain equilibrium in the radial direction near charged black branes with the hyperscaling violating factor. We explore the effect of the hyperscaling violating exponent θ and the dynamical parameter z. The influence

of the black brane temperature and NEC is also discussed. As shown in the previous section, we set $d = 2$, $\phi_0 = 0$, $Q = 2$, $r_h = 1$. The corresponding valid parameter space (θ, z) with the temperature T_H is shown in Fig. 2.

As shown in Fig. 2, when θ is a constant, the black brane temperature T_H decreases as z increases; when z is a constant, the black brane temperature T_H increases as θ increases. The red line in the figure shows the cases of $T_{\mu\nu}\xi^\mu\xi^\nu = 0$, and the NEC is violated below the red line. The points where z is smaller or θ is larger are closer to the region where the null energy condition is violated. To express our results more clearly, we discuss whether the chaos bound is violated by evaluating $\kappa^2 - \lambda^2$ numerically. When $\kappa^2 - \lambda^2 < 0$, the chaos bound $\lambda \leq \kappa$ is violated. The Lyapunov exponent λ is calculated by Eq. (25).

A. Fixed temperature T_H, varying θ, z

With fixed temperature T_H, but varying θ, z for the charged black branes, we first numerically analyze the relationship between the chaos bound and the Lyapunov exponent corresponding to the equilibrium in the radial direction. We consider the temperature of the black brane
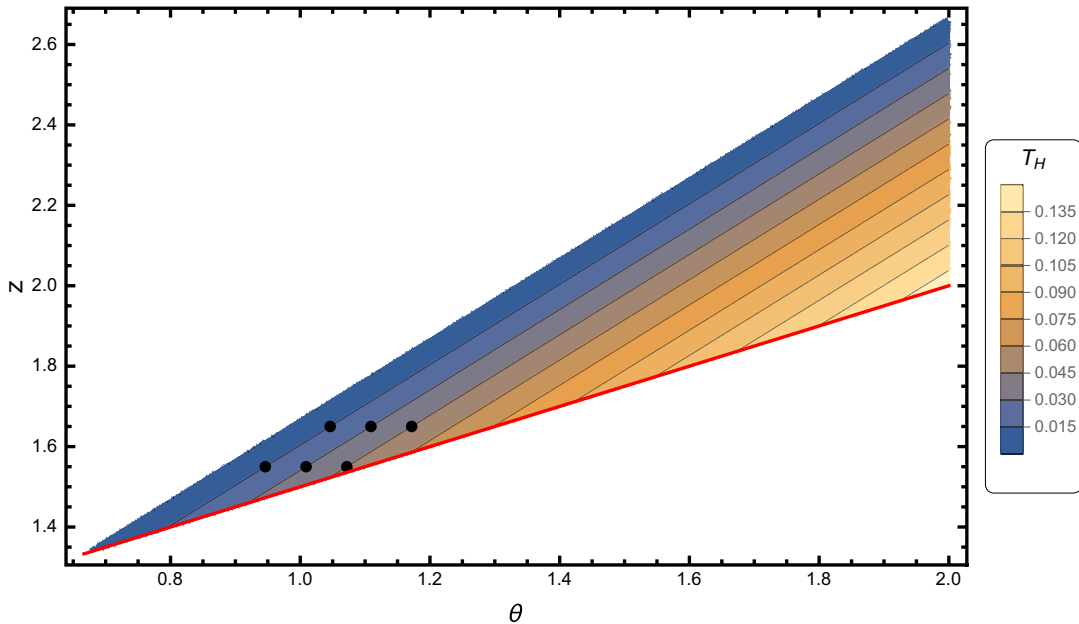

FIG. 2. The temperature T_H of the charged black brane as a function of the parameters θ and z. The black dots (θ, z) in the figure are the parameter values for the black branes that we discuss next subsection.
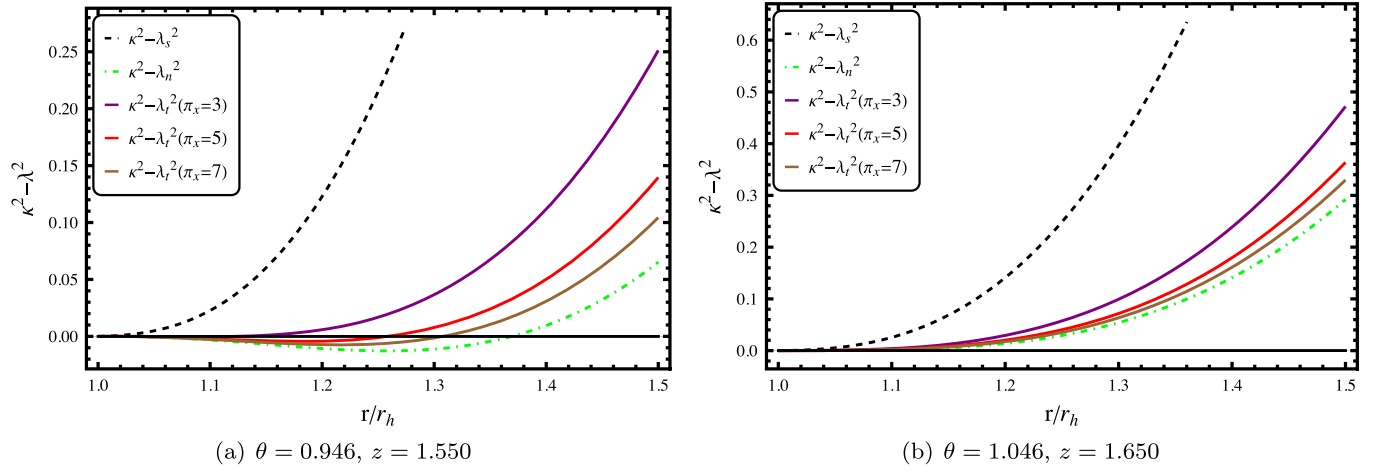
FIG. 3. $\kappa^2 - \lambda^2$ as a function of r/r_h near the charged black brane with (a) $\theta = 0.946$, $z = 1.550$ and (b) $\theta = 1.046$, $z = 1.650$ at $T_H = 0.015$. The chaos bound is violated in Fig. 3(a) since $\kappa^2 - \lambda^2 < 0$.

$T_H = 0.015$, 0.030, 0.045. The parameter values in the parameter space (θ, z) are shown in Fig. 2 with the black dots.

For a massive particle, we consider its static equilibrium (the lateral momentum $\pi_x = 0$) and the finite lateral momentum ($\pi_x = 3, 5, 7$). The Lyapunov exponent of null orbits is also considered, which equals to the value of timelike orbits with $\pi_x \to \infty$. The numerical results are presented in Figs. 3–5. In these figures, we use dashed lines to show the static equilibrium of a massive particle, dot-dashed lines to show the null orbits, and solid lines to show the results of the massive particle with finite lateral momentum ($\pi_x = 3, 5, 7$), respectively. $\kappa^2 - \lambda^2 < 0$ in these figures indicates that the chaos bound is violated by the test particle with equilibrium in the radial direction.

In Fig. 3, we plot the numerical results of $\kappa^2 - \lambda^2$ for the black brane temperature $T_H = 0.015$. We can see from Fig. 3(a) that there is $\kappa^2 - \lambda^2 < 0$ for λ_n and λ_t, which

indicates that the chaos bound is violated; while in Fig. 3(b) the chaos bound is not violated. This result indicates that the parameters θ and z affect the equilibrium stability of the test particles at the same temperature. The numerical results of $\kappa^2 - \lambda^2$ for the black brane temperature $T_H = 0.030$, 0.045 are plotted in Figs. 4 and 5, respectively. Similar to the case for $T_H = 0.015$, the chaos bound can be violated at the same temperature when θ and z are small. Meanwhile, comparing Figs. 3(a), 4(a) and 5(a), we can see that the higher temperature T_H is, the smaller the range r/r_h of the chaos bound violation is.

In Figs. 3–5, at the same equilibrium position, $\kappa^2 - \lambda^2$ decreases with the increase of the lateral momentum π_x of the test particle, then it indicates that the Lyapunov exponent of the timelike orbits becomes stronger with the increase of π_x. The Lyapunov exponent of the null orbits is the largest, which is consistent with our previous results of RN black holes [24]. In the charged black brane
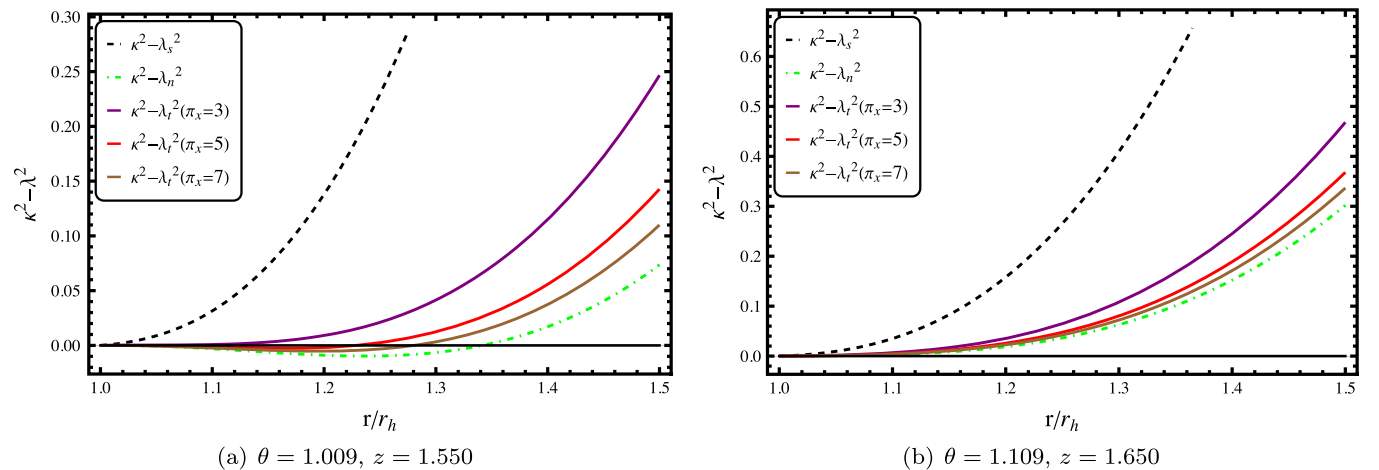

FIG. 4. $\kappa^2 - \lambda^2$ as a function of r/r_h near the charged black brane with (a) $\theta = 1.009$, $z = 1.550$ and (b) $\theta = 1.109$, $z = 1.650$ at $T_H = 0.030$. The chaos bound is violated for the green line in Fig. 4(a) since $\kappa^2 - \lambda^2 < 0$.

(a) $\theta = 1.072$, $z = 1.550$

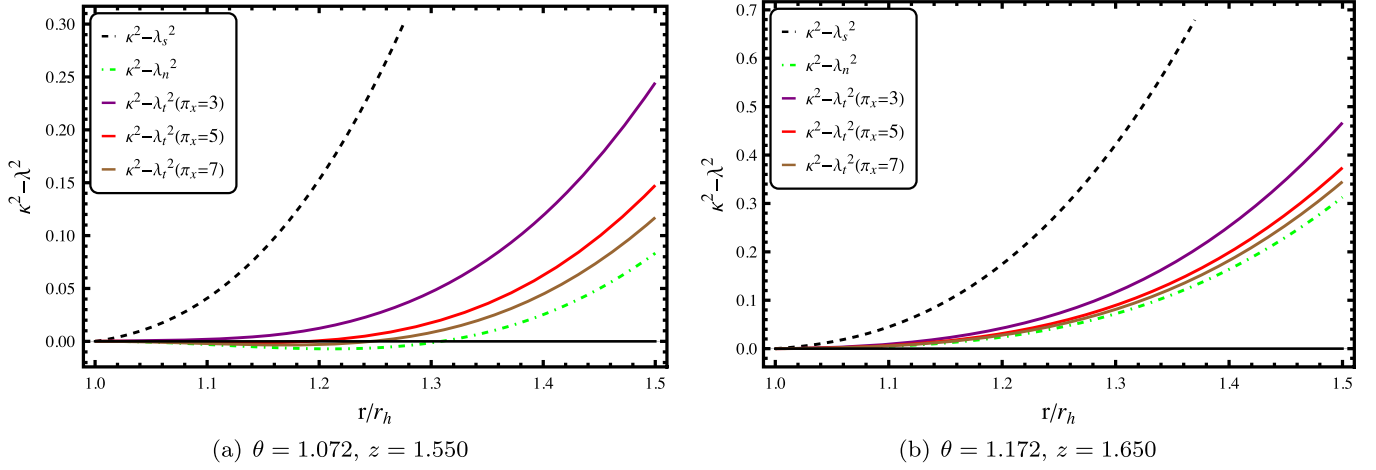(b) $\theta = 1.172$, $z = 1.650$

FIG. 5. $\kappa^2 - \lambda^2$ as a function of r/r_h near the charged black brane with (a) $\theta = 1.072$, $z = 1.550$ and (b) $\theta = 1.172$, $z = 1.650$ at $T_H = 0.045$. The chaos bound is violated for the green line in Fig. 5(a) since $\kappa^2 - \lambda^2 < 0$.

(a) $\theta = 0.80$

(b) $\theta = 1.10$

(c) $\theta = 1.50$

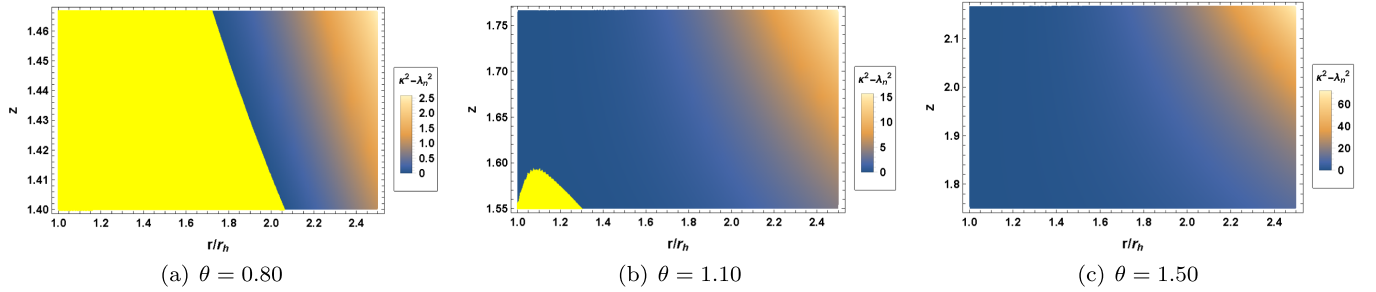FIG. 6. The contour plot of $\kappa^2 - \lambda_n^2$ as a function of z and r/r_h for fixed θ: (a) $\theta = 0.80$, (b) $\theta = 1.10$ and (c) $\theta = 1.50$. The yellow region corresponds to the chaos bound violated region.

background, the parameters of the black brane, in addition to the temperature, also affect whether the chaos bound is violated.

Next, we will further discuss the relationship between the black brane parameters and the Lyapunov exponent of the test particle with equilibrium in the radial direction. We discuss the null orbit because it has the largest Lyapunov exponent and is most likely to exceed the bound $\lambda \leq \kappa$.

B. Fixed parameter θ or z

To explore the relationship between the black brane parameters and the Lyapunov exponent of particle motion, here we investigate the null orbits of the test particle at the same black brane parameter θ and z, respectively. The numerical results for $\kappa^2 - \lambda_n^2$ are shown in Figs. 6 and 7, with the colored region where $\kappa^2 - \lambda_n^2 > 0$. The region where $\kappa^2 - \lambda_n^2 < 0$ is marked in yellow in these plots, which indicates that the chaos bound is violated.

In Fig. 6, the numerical results of $\kappa^2 - \lambda_n^2$ for null orbits are shown, which has three plots for different $\theta = 0.80$, 1.10, 1.50. For each plot, the horizontal axis represents r/r_h, and the vertical axis represents the parameter z.

For the plot with $\theta = 0.80$ in Fig. 6(a), all available values of z have yellow regions, which means that the chaos bound is always violated. As z increases, there is a decrease in the range of r/r_h where the chaos bound can be violated. In Fig. 6(b), we show that for $\theta = 1.10$, the chaos bound can be violated near the minimal value of z, and the region where the chaos bound is violated decreases as z increases. The minimal value of z corresponds to the zero-temperature of the charged black brane. There is no violation of the chaos bound as shown in Fig. 6(c).

For $z = 1.40$, 1.59, 2.10, the results of $\kappa^2 - \lambda^2$ are shown in Fig. 7. The horizontal axis represents r/r_h, and the vertical axis represents the parameter θ. We color the region in yellow where the chaos bound is violated. As shown in Fig. 7(a) with $z = 1.40$, the chaos bound is violated for all values of θ. In Fig. 7(b), there is $\theta = 1.59$. The chaos bound can be violated in two regions close to the maximal and minimal values of θ. The maximal and minimal values of θ correspond to the cases of $T_{\mu\nu}\xi^\mu\xi^\nu = 0$ and the zero-temperature, respectively. The range r/r_h of the violation of chaos bound is larger near the maximal and minimal values of θ. The chaos bound is not violated for the plot with $\theta = 2.10$ in Fig. 7(c).
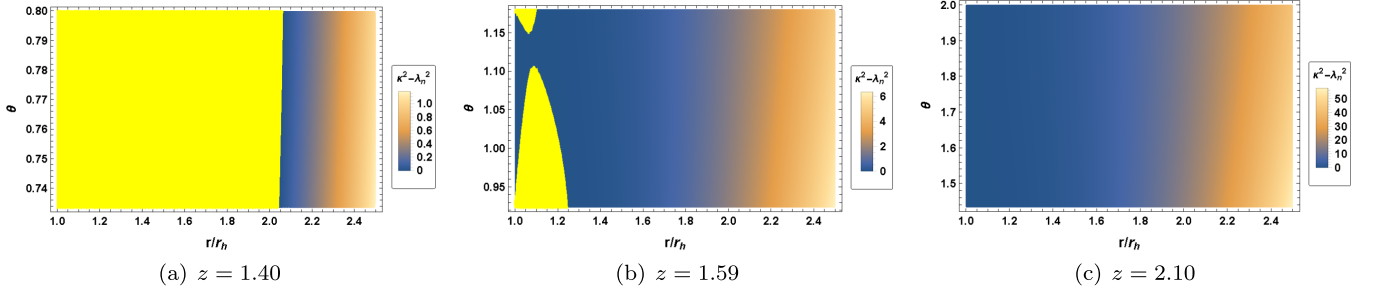
FIG. 7. The contour plot of $\kappa^2 - \lambda_n^2$ as a function of θ and r/r_h for fixed z: (a) $z = 1.40$, (b) $z = 1.59$ and (c) $z = 2.10$. The yellow region corresponds to the chaos bound violated region.
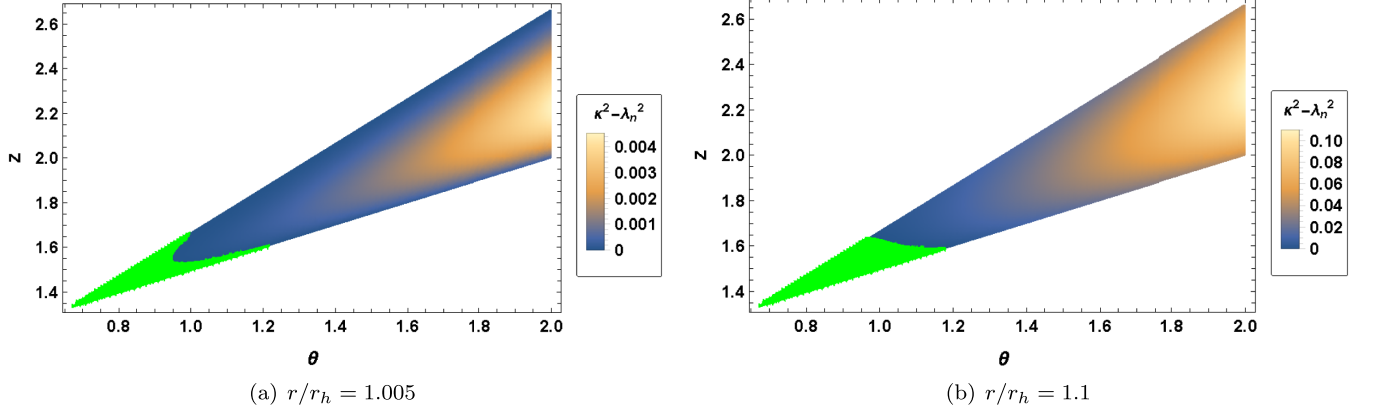

FIG. 8. The contour plot of $\kappa^2 - \lambda_n^2$ as a function of θ and z for fixed r/r_h: (a) $r/r_h = 1.005$, (b) $r/r_h = 1.1$. The green region corresponds to the parameter space (θ, z) where the chaos bound is violated.

From Figs. 6 and 7, we can conclude these results. There is always $\kappa^2 - \lambda_n^2 < 0$ when θ and z are small, as in Figs. 6(a) and 7(a). We can see that in Figs. 6(b)[1] and 7(b), as θ and z increase, the violation of chaos bound only exists in the parameter range near the zero-temperature and the critical values of NEC. The range of r/r_h with $\kappa^2 - \lambda_n^2 < 0$ is the biggest at the extremal cases of temperature and NEC. As θ and z deviate from the extremal cases, the range r/r_h of $\kappa^2 - \lambda_n^2 < 0$ decreases. In Figs. 6(b) and 7(b), around the equilibrium position $r/r_h = 1.1$, there is a maximal range of parameters that can violate $\lambda \leq \kappa$. In Figs. 6(c) and 7(c), $\kappa^2 - \lambda_n^2$ is always positive. There seems to be no more $\kappa^2 - \lambda_n^2 < 0$ once θ and z are large enough.

From these results, we can see that the violation of the chaos bound is influenced by the parameters θ and z near the charged black brane, and the chaos bound is easily violated when θ and z are small. Also, we can see that the chaos bound is also easily violated near the zero-temperature and the critical values of the null energy

condition, which reveals the relationship between the particle motion instability and the black brane's parameters, temperature and the null energy condition.

C. Fixed equilibrium position r/r_h

To show more clearly the effect of the temperature and the null energy condition on the chaos bound, we analyze $\kappa^2 - \lambda_n^2$ for the fixed radial position r/r_h where the test particle maintains equilibrium in the radial direction.

In Fig. 8, the numerical result of $\kappa^2 - \lambda_n^2$ as a function of θ and z for fixed r/r_h is plotted. The case of $r/r_h = 1.005$ is considered because it is near the horizon. In the previous subsection, we can see that the violation of the chaos bound is often located at $r/r_h = 1.1$, so we also consider the case of $r/r_h = 1.1$. The region where $\kappa^2 - \lambda_n^2 < 0$ is colored in green, which means the bound $\lambda \leq \kappa$ is violated.

The numerical results at the equilibrium position $r/r_h = 1.005$ are shown in Fig. 8(a). There is always $\kappa^2 - \lambda_n^2 < 0$ in the region where the parameters θ and z are small. However, as the parameters increase, $\kappa^2 - \lambda_n^2 < 0$ can be seen only in the parameter space near the zero-temperature and the cases of $T_{\mu\nu}\xi^\mu\xi^\nu = 0$. The maximal value of $\theta = 1.217$ for the violation of chaos bound at $r/r_h = 1.005$ is given by $T_{\mu\nu}\xi^\mu\xi^\nu = 0$, and another parameter maximal

---

[1]In this plot, there is no $\kappa^2 - \lambda_n^2 < 0$ near the zero-temperature. This is probably because z is already greater than some critical value. In the next discussion, there will be more intuitive results to show that λ_n is more likely to exceed $\lambda \leq \kappa$ near extremal black branes.

value $z = 1.665$ is given by the zero-temperature limit. In Fig. 8(b), the result at the position $r/r_h = 1.1$ shows that $\kappa^2 - \lambda_n^2 < 0$ exists in the small parameter region (θ, z). Something is different in that there is still $\kappa - \lambda_n^2 < 0$ even in the middle parameter region. In this case, the maximal values of the parameters satisfying $\kappa^2 - \lambda_n^2 < 0$ are $\theta = 1.179$ and $z = 1.634$, which are smaller than Fig. 8(a).

In Fig. 8 we can see that the value of $\kappa - \lambda_n^2$ is always smaller near the upper and lower boundary of the parameter space. The maximal parameter values that allow $\kappa - \lambda_n^2 < 0$ also always appear on the upper and lower boundary of the parameter space. The upper and lower boundary corresponds to the cases of the zero-temperature $T_H = 0$ and $T_{\mu\nu}\xi^\mu\xi^\nu = 0$, respectively. This suggests a connection between the Lyapunov exponent in the particle motion and the black brane temperature as well as the NEC. We can obtain the critical parameters θ_c and z_c for $\kappa - \lambda_n^2 < 0$ in the cases of zero-temperature and critical values of NEC. These parameters θ_c and z_c provide the possibility of the violation of chaos bound, i.e., the bound $\lambda \leq \kappa$ cannot be violated by test particles with equilibrium in the radial direction when $\theta > \theta_c$ and $z > z_c$.

V. THE CRITICAL PARAMETERS θ_c AND z_c FOR THE VIOLATION OF $\lambda \leq \kappa$

In the previous section, we discussed the bound of test particles' equilibrium in the radial direction and found the violation. The effect of the black brane temperature T_H and the null energy condition (NEC) is investigated. The results showed that the bound $\lambda \leq \kappa$ is more likely to be violated near the cases of zero-temperature black branes and the critical value of NEC ($T_{\mu\nu}\xi^\mu\xi^\nu = 0$).[2] Through the investigation of zero-temperature cases and the cases of $T_{\mu\nu}\xi^\mu\xi^\nu = 0$, we can understand more about the violation of chaos bound in the charged black brane with the hyperscaling violating factor and find the critical parameters (θ_c and z_c) for the violation of chaos bound. When $\theta > \theta_c$ or $z > z_c$, the bound $\lambda \leq \kappa$ is always satisfied.

As before, we set the parameters $d = 2$, $\phi_0 = 0$, $Q = 2$ and $r_h = 1$ in Eq. (4). We investigate whether the equilibrium in the radial direction of test particles violates the upper bound of the Lyapunov exponent λ based on the value of $\kappa^2 - \lambda^2$, and the bound is violated when $\kappa^2 - \lambda^2 < 0$.

A. $T_H = 0$ case

We consider the extremal black brane with $T_H = 0$ and explore the violation of bound in test particles' equilibrium in the radial direction. From Eq. (10), we can obtain the zero-temperature condition

---

[2]The null energy condition (NEC) means $T_{\mu\nu}\xi^\mu\xi^\nu \geq 0$, so we call the case of $T_{\mu\nu}\xi^\mu\xi^\nu = 0$ as the critical value for the violation of NEC.

$$z - \theta = \frac{2}{3}. \qquad (27)$$

Near the extremal charged black brane, the Lyapunov exponent λ_n of null orbits can be reduced to the form related to θ or z, respectively. We can obtain the formula of $\kappa^2 - \lambda_n^2$ in terms of θ as

$$\kappa^2 - \lambda_n^2 = \frac{1}{9}r^{2\theta - \frac{16}{3}}(48(8 - 10\theta + 3\theta^2) + 75r^{\frac{4}{3}}(5 - 8\theta + 3\theta^2)$$
$$+ 24r^{\frac{10}{3}}(8 - 5\theta + 3\theta^2) - 30r^4(5 - 4\theta + 3\theta^2) + r^{\frac{20}{3}}$$
$$\times (9\theta^2 - 1) - 40r^{\frac{2}{3}}(20 - 27\theta + 9\theta^2)), \qquad (28)$$

and the formula in terms of z as

$$\kappa^2 - \lambda_n^2 = \frac{1}{9}r^{2z - \frac{20}{3}}(48(16 - 14z + 3z^2) - 120r^{\frac{2}{3}}(14 - 13z + 3z^2)$$
$$- 30r^4(9 - 8z + 3z^2) + 3r^{\frac{20}{3}}(1 - 4z + 3z^2) + 25r^{\frac{4}{3}}$$
$$\times (35 - 26z + 9^2) + 8r^{\frac{10}{3}}(38 - 27z + 9z^2)). \qquad (29)$$

In Fig. 9, we show the numerical results of $\kappa^2 - \lambda_n^2$ in the extremal charged black brane. The region where the chaos bound is violated is colored in yellow. As shown in the two plots, the range of r/r_h for the violation of the bound decreases with the increase of θ (or z) until the chaos bound is no longer violated near the horizon. There are obviously the critical parameter values θ_c and z_c, and when $\theta > \theta_c$ (or $z > z_c$), there is no $\kappa^2 - \lambda_n^2 < 0$.

To find the critical values of parameters (θ and z), we expand Eqs. (28) and (29) near the horizon ($r_h = 1$). There are

$$\kappa^2 - \lambda_n^2 \sim (\theta - 1)(r - 1)^3 + \mathcal{O}((r - 1)^4), \qquad (30)$$

and

$$\kappa^2 - \lambda_n^2 \sim (3z - 5)(r - 1)^3 + \mathcal{O}((r - 1)^4). \qquad (31)$$

From the above equations, we can obtain the critical values for the violation of chaos bound in the extremal charged black brane, which we denote here as θ_{c1} and z_{c1}, respectively: $\theta_{c1} = 1$ and $z_{c1} = 5/3$.

B. $T_{\mu\nu}\xi^\mu\xi^\nu = 0$ case

Next, we discuss the chaos bound at $T_{\mu\nu}\xi^\mu\xi^\nu = 0$. In the previous discussion, our results show that $\kappa^2 - \lambda^2 < 0$ is more likely to happen at the parameter range satisfying of $T_{\mu\nu}\xi^\mu\xi^\nu = 0$. Here we focus on the charged black brane with the constraint $T_{\mu\nu}\xi^\mu\xi^\nu = 0$. With the null energy condition Eq. (12), the black brake parameters are constrained by

$$2z - \theta = 2. \qquad (32)$$

(a) $\kappa^2 - \lambda_n^2$ as the function of r/r_h and θ

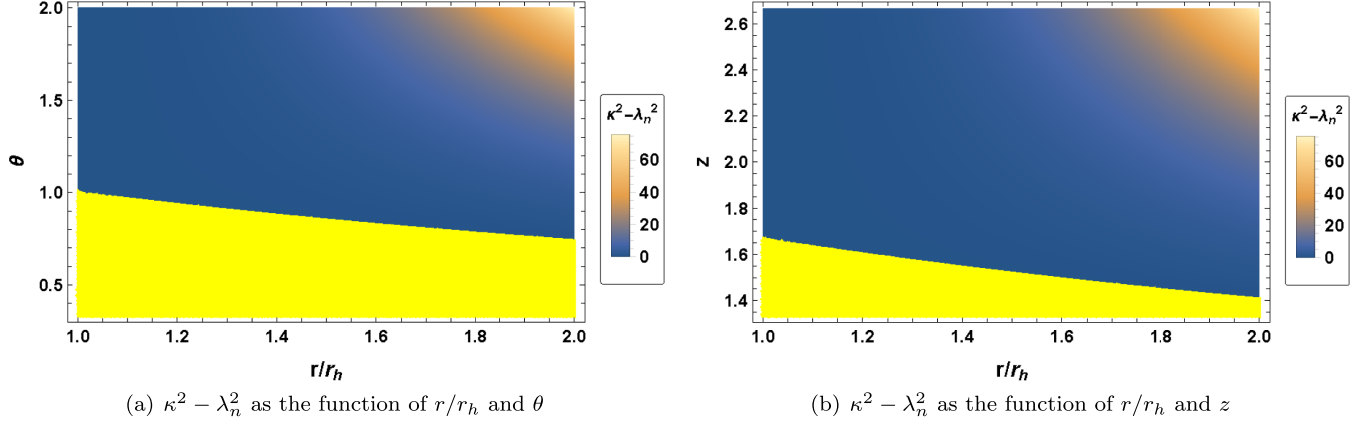(b) $\kappa^2 - \lambda_n^2$ as the function of r/r_h and z

FIG. 9.   The contour plot of $\kappa^2 - \lambda_n^2$ in the extremal charged black brane: (a) $\kappa^2 - \lambda_n^2$ as the function of r/r_h and θ, (b) $\kappa^2 - \lambda_n^2$ as the function of r/r_h and z. In the yellow region, $\kappa^2 - \lambda_n^2 < 0$, which means the bound $\lambda \leq \kappa$ is violated.

In the critical cases of NEC $T_{\mu\nu}\xi^\mu\xi^\nu = 0$, we can simplify the expression of $\kappa^2 - \lambda_n^2$ in terms of θ as

$$\kappa^2 - \lambda_n^2 = \frac{1}{16}(2-3\theta)^2 + \frac{75}{16}r^{2\theta-4}(\theta-2)^2 - 15r^{\frac{5\theta}{2}-5} + 8r^{3\theta-6}$$

$$\times (\theta-2)^2 + \frac{1}{4}r^{\theta-2}(2\theta r^4 - 5r^{1+\frac{\theta}{2}}(12+\theta(\theta-4))$$

$$+ 4r^\theta(24+\theta(3\theta-14))), \tag{33}$$

and the formula of $\kappa^2 - \lambda_n^2$ in terms of θ as

$$\kappa^2 - \lambda_n^2 = \frac{1}{4}(4-3z)^2 - 60r^{5(z-2)}(z-2)^2 + 32r^{6(z-2)}(z-2)^2$$

$$+ \frac{75}{4}r^{4z-8}(z-2)^2 + r^{2z}(r^{2z-6}(64+4z(3z-13))$$

$$- 5r^{z-4}(6+z(z-4))+z-1). \tag{34}$$

We show the results of Eqs. (33) and (34) in Fig. 10, and there is $\kappa^2 - \lambda_n^2 < 0$ in the yellow region. For the charged black brane with the critical values of NEC, we can see in

Fig. 10 that the region of $\kappa^2 - \lambda_n^2 < 0$ in r/r_h shrinks as θ (or z) increases until there is no $\kappa^2 - \lambda_n^2$ near the horizon.

Near the horizon $r_h = 1$, we can expand Eqs. (33) and (34) as

$$\kappa^2 - \lambda_n^2 = \left(\frac{33}{2} - 50\theta + 50\theta^2 - \frac{81}{4}\theta^3 + \frac{99}{32}\theta^4\right)(r-1)^2$$

$$+ \mathcal{O}(r-1)^3, \tag{35}$$

and

$$\kappa^2 - \lambda_n^2 = \frac{1}{2}(3z-4)(z(394+z(33z-196))-264)$$

$$\times (r-1)^2 + \mathcal{O}(r-1)^3. \tag{36}$$

The critical values θ_{c2} and z_{c2} for the violation of chaos bound in the cases of $T_{\mu\nu}\xi^\mu\xi^\nu = 0$ are $\theta_{c2} = 1.219$ and $z_{c2} = 1.610$. These values are related to the null energy condition (NEC).

(a) $\kappa^2 - \lambda_n^2$ as the function of r/r_h and θ

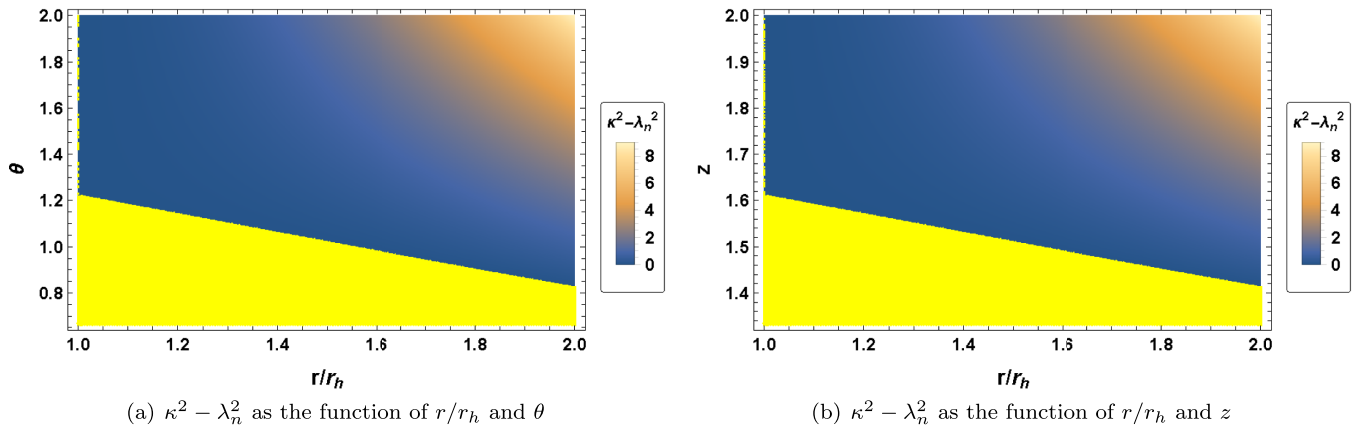(b) $\kappa^2 - \lambda_n^2$ as the function of r/r_h and z

FIG. 10.   The contour plot of $\kappa^2 - \lambda_n^2$ in the charged black brane with $T_{\mu\nu}\xi^\mu\xi^\nu = 0$: (a) $\kappa^2 - \lambda_n^2$ as the function of r/r_h and θ, (b) $\kappa^2 - \lambda_n^2$ as the function of r/r_h and z. In the yellow region, $\kappa^2 - \lambda_n^2 < 0$, corresponds to the chaos bound $\lambda \leq \kappa$ violated area.

The larger values of θ_{c1} and θ_{c2} (z_{c1} and z_{c2}) are the critical parameter values: $\theta_c = \text{Max}(\theta_{c1}, \theta_{c2})$ and $z_c = \text{Max}(z_{c1}, z_{c2})$. For our setting of parameters ($d = 2$, $\phi_0 = 0$, $Q = 2$ and $r_h = 1$), the critical parameters are $\theta_c = 1.219$ and $z_c = 5/3$. In the parameter space (θ, z) where $\theta > \theta_c$ or $z > z_c$, $\kappa^2 - \lambda_n^2$ is always positive, which means the chaos bound is satisfied.[3]

VI. CONCLUSION

In summary, we investigate the Lyapunov exponent of a test particle near the charged black branes with the hyperscaling violating factor. The Lyapunov exponent of particle motion near the horizon has an upper bound, which equals the surface gravity κ and is called the chaos bound [21,22]. The relationship between the equilibrium in the radial direction of test particles and the chaos bound is discussed here. Considering different parameters of the black brane, we find the violation of the chaos bound. Whether the chaos bound can be violated is related to the black brane parameters (θ and z), the black brane temperature T_H, and the null energy condition (NEC).

We study the effects of different parameters θ and z on the particle motion near the black brane, while in our previous work, we pointed out the relationship between the black hole temperature and the chaos bound in the particle motion. The Lyapunov exponent of test particles' equilibrium in the radial direction can be obtained from the Jacobian matrix. The results show that even at the same temperature T_H, the test particle still has different behavior of the Lyapunov exponent. Obviously, this is the effect of black brane parameters θ and z. For the equilibrium of test particles, its Lyapunov exponent increases with the lateral momentum. Considering timelike orbits, in the limit where the lateral momentum converges to infinity, the Lyapunov exponent converges to the value of null orbits. Therefore we discuss the Lyapunov exponent λ_n of the null orbits and the surface gravity κ to study the bound $\lambda \le \kappa$, since it is most likely to be beyond the bound. We analyze the numerical results of $\kappa^2 - \lambda_n^2$ for the same parameters θ and z. The results show that when the hyperscaling violating exponent θ and the dynamical exponent z are small, there is always $\kappa^2 - \lambda_n^2 < 0$. As θ and z increase, the parameter space $\theta - z$ which has $\kappa^2 - \lambda_n^2 < 0$ becomes smaller, and $\kappa - \lambda_n^2 < 0$ only exists in the region near the zero-temperature cases and the cases of $T_{\mu\nu}\xi^\mu\xi^\nu = 0$. As the parameters continue to increase, there is no violation of $\lambda \le \kappa$. These results illustrate that the zero-temperature as well as the violation of NEC gives more possibilities of violating the chaos bound. By considering the limiting examples

of zero-temperature and the cases of $T_{\mu\nu}\xi^\mu\xi^\nu = 0$, we obtain the critical parameters θ_c and z_c. The bound $\lambda \le \kappa$ is always satisfied by the equilibrium in the radial direction of test particles when $\theta > \theta_c$ or $z > z_c$. The critical parameters imply a potential connection between the violation of bound $\lambda \le \kappa$ and the properties of spacetime. This connection is demonstrated in the Hawking temperature and null energy condition. Note that the results can recover that of RN-AdS black hole when $z = 1$ and $\theta = 0$. However, due to the complicated influence of parameters θ and z on the background spacetime, we do not see a significant difference in the geometry as the parameters are above or below these critical parameters. The relationship between the Lyapunov exponent's upper bound in particle motion and space-time geometry does require further investigation and exploration.

We obtain the violation of the bound $\lambda \le \kappa$ in the charged black brane with the hyperscaling violating factor. This result may not be contrary to the conjecture $\lambda \le 2\pi T/\hbar$ proposed in [15], since the conjecture was obtained from the out-of-time-order correlator (OTOC) in quantum systems. In holographic theory, it is recognized that OTOC in quantum field theory is dual to the shock wave at the horizon. It is clear that the single particle motion we are discussing is different from the shock wave. At the horizon, $\lambda = \kappa$ is always satisfied. However, it is still interesting to study the Lyapunov exponent in particle motion and the violation of the bound. In the study on the Lyapunov exponent of particle motion, some interesting conjectures have been proposed. Such as the relationship between the Lyapunov exponent of particle motion, the energy bound [42] and the causality bound [43]. Guo *et al.* probed the connection between the black hole phase transitions and the Lyapunov exponents of particle motion [44]. Recently, the relationship between the test particles' homoclinic orbits and chaos bound in the black hole with anisotropic matter fields has also been discussed [45]. More about the connection between the chaos bound and the nature of black holes remains to be uncovered.

Our work supports the contact between the violation of the chaos bound and the properties of the black brane (the Hawking temperature and the null energy condition). These results illustrate the potential physical significance of the violation of the chaos bound in particle motion. It will be of great interest to study more about the dynamic stability of black holes through the chaos bound in the particle motion, because there is an intrinsic correlation between them, and figuring out this correlation will help us further understand the black hole.

---

[3]In the appendix, we consider the spacetime with the violation of NEC. In the parameter space (θ, z) larger than the critical parameters θ_c and z_c, the violation of chaos bound still exists. This implies that a deeper physical meaning exists between the chaos bound and the NEC.

APPENDIX: THE BLACK BRANES WITH THE VIOLATION OF NEC

With the parameters

$$d = 2, \qquad \phi_0 = 0, \qquad Q = 2, \qquad r_h = 1,$$

we consider the black branes where NEC is violated. The temperature T_H at the horizon can be obtained by the parameters θ and z, and we show it in Fig. 11. We can see that T_H at the horizon increases as θ increases and decreases as z increases.

To explore whether the chaos bound can be violated, we compute the value of $\kappa^2 - \lambda_n^2$, and if $\kappa^2 - \lambda_n^2 < 0$, it means that the chaos bound is violated. We plot the numerical results of $\kappa^2 - \lambda_n^2$ in Fig. 12, which has three plots for different equilibrium positions $r/r_h = 1.0001, 1.005, 1.1$. In the colored region, $\kappa^2 - \lambda_n^2 < 0$, the chaos bound is violated. And the region where $\kappa^2 - \lambda_n^2 > 0$ is marked in gray.

As shown in Fig. 12, in the background where NEC is violated, there is $\kappa^2 - \lambda_n^2 < 0$ in most parameter space (θ, z). For the equilibrium position $r/r_h = 1.0001$ in Fig. 12(a), $\kappa^2 - \lambda_n^2 < 0$ always exists. This result means that in spacetime with the violation of NEC, the chaos bound can always be violated. The results at the equilibrium position $r/r_h = 1.005, 1.1$ are shown in Figs. 12(b) and 12(c), respectively. $\kappa^2 - \lambda_n^2$ can be positive only when θ and z are large and close to the cases of $T_{\mu\nu}\xi^\mu\xi^\nu = 0$. The closer the equilibrium position is to the horizon, the smaller the range of $\kappa^2 - \lambda_n^2 > 0$. It is worth noting that in black brane with the violation of NEC, the chaos bound is still violated when $\theta > \theta_c$ (or $z > z_c$). This implies an intrinsic relationship between the Lyapunov exponent in particle motion and the null energy condition, and it also reminds us of the possible relevance of the chaos bound in particle motion to some interesting questions, such as the instability of spacetime and the causality.
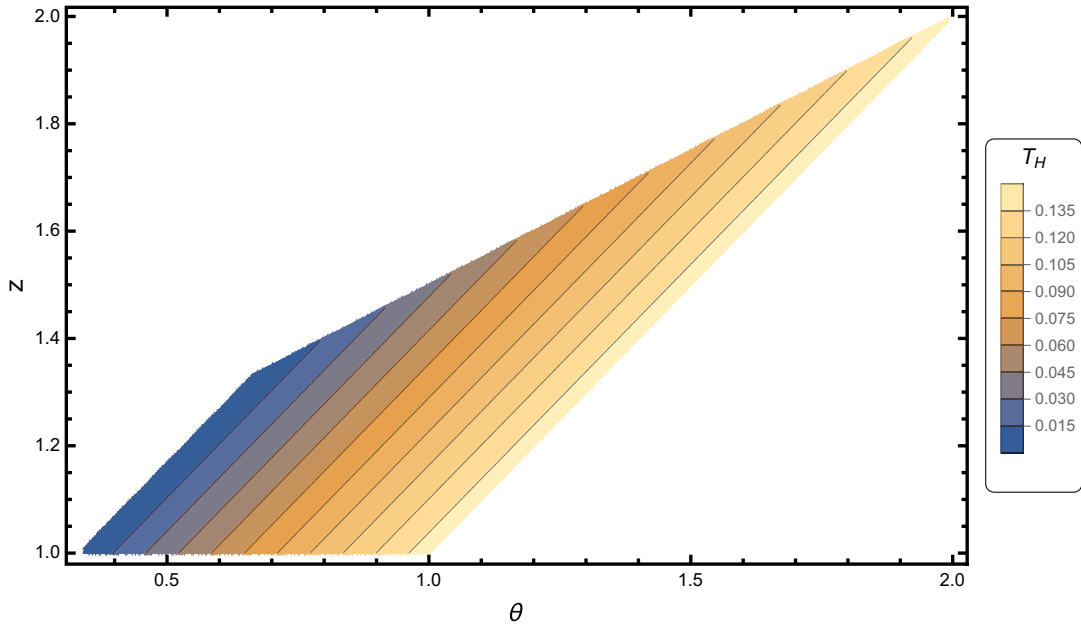

FIG. 11.   The temperature T_H of the black branes with the violation of NEC as a function of the parameters θ and z.
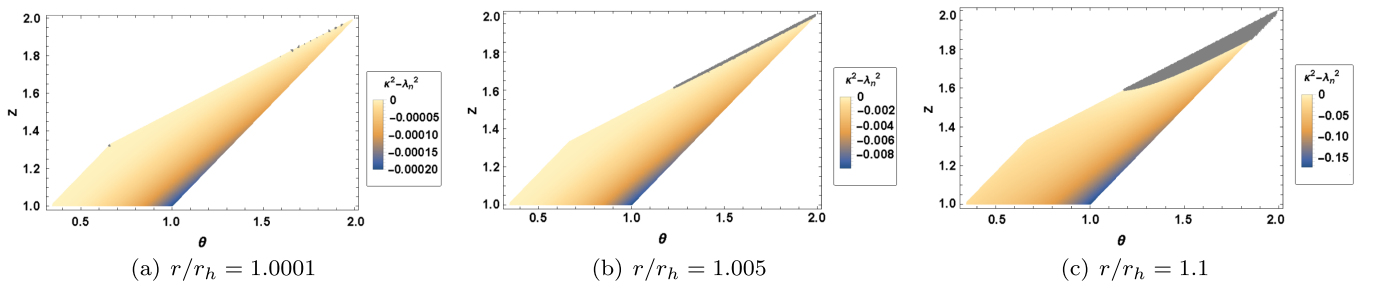

(a) $r/r_h = 1.0001$ (b) $r/r_h = 1.005$ (c) $r/r_h = 1.1$

FIG. 12.   The contour plot of $\kappa^2 - \lambda_n^2$ as a function of θ and z for fixed r/r_h: (a) $r/r_h = 1.0001$, (b) $r/r_h = 1.005$, (c) $r/r_h = 1.1$. The colored region in these three plots denotes that $\kappa^2 - \lambda_n^2 < 0$, which means the bound $\lambda \leq \kappa$ is violated. The region which means $\kappa^2 - \lambda_n^2 > 0$ is marked in gray.

[1] S. Suzuki and K.-i. Maeda, Chaos in Schwarzschild space-time: The motion of a spinning particle, Phys. Rev. D **55,** 4848 (1997).

[2] P. S. Letelier and W. M. Vieira, Chaos and rotating black holes with halos, Phys. Rev. D **56,** 8095 (1997).

[3] A. P. S. de Moura and P. S. Letelier, Chaos and fractals in geodesic motions around a nonrotating black hole with an external halo, Phys. Rev. E **61,** 6506 (2000).

[4] J. K. Kao and H. T. Cho, The Onset of chaotic motion of a spinning particle around the Schwarzschild black hole, Phys. Lett. A **336,** 159 (2005).

[5] S. Chen, M. Wang, and J. Jing, Chaotic motion of particles in the accelerating and rotating black holes spacetime, J. High Energy Phys. 09 (2016) 082.

[6] M. Wang, S. Chen, and J. Jing, Chaos in the motion of a test scalar particle coupling to the Einstein tensor in Schwarzschild–Melvin black hole spacetime, Eur. Phys. J. C **77,** 208 (2017).

[7] D.-Z. Ma, J.-P. Wu, and J. Zhang, Chaos from the ring string in a Gauss-Bonnet black hole in AdS_5 space, Phys. Rev. D **89,** 086011 (2014).

[8] A. Bera, S. Dalui, S. Ghosh, and E. C. Vagenas, Quantum corrections enhance chaos: Study of particle motion near a generalized Schwarzschild black hole, Phys. Lett. B **829,** 137033 (2022).

[9] J. Xie, Y. Wang, and B. Tang, Chaotic dynamics of string around the Bardeen-AdS black holes surrounded by quintessence dark energy, Phys. Dark Universe **40,** 101184 (2023).

[10] M. Chabab, H. El Moumni, S. Iraoui, K. Masmar, and S. Zhizeh, Chaos in charged AdS black hole extended phase space, Phys. Lett. B **781,** 316 (2018).

[11] S. Mahish and B. Chandrasekhar, Chaos in charged Gauss-Bonnet AdS black holes in extended phase space, Phys. Rev. D **99,** 106012 (2019).

[12] Y. Chen, H. Li, and S.-J. Zhang, Chaos in Born–Infeld–AdS black hole within extended phase space, Gen. Relativ. Gravit. **51,** 134 (2019).

[13] C. Dai, S. Chen, and J. Jing, Thermal chaos of a charged dilaton-AdS black hole in the extended phase space, Eur. Phys. J. C **80,** 245 (2020).

[14] X. Zhou, Y. Xue, B. Mu, and J. Tao, Temporal and spatial chaos of RN-AdS black holes immersed in perfect fluid dark matter, Phys. Dark Universe **39,** 101168 (2023).

[15] J. Maldacena, S. H. Shenker, and D. Stanford, A bound on chaos, J. High Energy Phys. 08 (2016) 106.

[16] S. H. Shenker and D. Stanford, Black holes and the butterfly effect, J. High Energy Phys. 03 (2014) 067.

[17] S. H. Shenker and D. Stanford, Multiple shocks, J. High Energy Phys. 12 (2014) 046.

[18] R. R. Poojary, BTZ dynamics and chaos, J. High Energy Phys. 03 (2020) 048.

[19] V. Jahnke, K.-Y. Kim, and J. Yoon, On the chaos bound in rotating black holes, J. High Energy Phys. 05 (2019) 037.

[20] Y. Liu and A. Raju, Quantum chaos in topologically massive gravity, J. High Energy Phys. 12 (2020) 027.

[21] K. Hashimoto and N. Tanahashi, Universality in chaos of particle motion near black hole horizon, Phys. Rev. D **95,** 024007 (2017).

[22] Q.-Q. Zhao, Y.-Z. Li, and H. Lu, Static equilibria of charged particles around charged black holes: Chaos bound and its violations, Phys. Rev. D **98,** 124001 (2018).

[23] Y.-Q. Lei, X.-H. Ge, and C. Ran, Chaos of particle motion near a black hole with quasitopological electromagnetism, Phys. Rev. D **104,** 046020 (2021).

[24] Y.-Q. Lei and X.-H. Ge, Circular motion of charged particles near a charged black hole, Phys. Rev. D **105,** 084011 (2022).

[25] N. Kan and B. Gwak, Bound on the Lyapunov exponent in Kerr-Newman black holes via a charged particle, Phys. Rev. D **105,** 026006 (2022).

[26] B. Gwak, N. Kan, B.-H. Lee, and H. Lee, Violation of bound on chaos for charged probe in Kerr-Newman-AdS black hole, J. High Energy Phys. 09 (2022) 026.

[27] C. Yu, D. Chen, and C. Gao, Bound on Lyapunov exponent in Einstein-Maxwell-dilaton-axion black holes, Chin. Phys. C **46,** 125106 (2022).

[28] C. Gao, D. Chen, C. Yu, and P. Wang, Chaos bound and its violation in charged Kiselev black hole, Phys. Lett. B **833,** 137343 (2022).

[29] D. Chen and C. Gao, Angular momentum and chaos bound of charged particles around Einstein–Euler–Heisenberg AdS black holes, New J. Phys. **24,** 123014 (2022).

[30] R. Yin, J. Liang, and B. Mu, Chaos bound and its violation in the torus-like black hole, arXiv:2210.07799.

[31] Y. Song, R. Yin, Y. He, and B. Mu, Chaos bound of charged particles around phantom AdS black hole, arXiv:2211.04990.

[32] D. Chen and C. Gao, Chaos bound in Kerr-Newman-Taub-NUT black holes via circular motions*, Chin. Phys. C **47,** 015108 (2023).

[33] D. Giataganas, Chaotic motion near black hole and cosmological horizons, Fortschr. Phys. **70,** 2200001 (2022).

[34] M. Alishahiha, E. O Colgain, and H. Yavartanoo, Charged black branes with hyperscaling violating factor, J. High Energy Phys. 11 (2012) 137.

[35] X.-H. Ge, Y. Tian, S.-Y. Wu, and S.-F. Wu, Hyperscaling violating black hole solutions and Magneto-thermoelectric DC conductivities in holography, Phys. Rev. D **96,** 046015 (2017); **97,** 089901(E) (2018).

[36] X.-H. Ge, Y. Tian, S.-Y. Wu, S.-F. Wu, and S.-F. Wu, Linear and quadratic in temperature resistivity from holography, J. High Energy Phys. 11 (2016) 128.

[37] X.-H. Ge, S.-J. Sin, Y. Tian, S.-F. Wu, and S.-Y. Wu, Charged BTZ-like black hole solutions and the diffusivity-butterfly velocity relation, J. High Energy Phys. 01 (2018) 068.

[38] X.-H. Ge, Y. Seo, S.-J. Sin, and G. Song, New black holes with hyperscaling violation for the transports of quantum critical points with magnetic impurity, J. High Energy Phys. 06 (2020) 128.

[39] V. Cardoso, A. S. Miranda, E. Berti, H. Witek, and V. T. Zanchin, Geodesic stability, Lyapunov exponents and quasinormal modes, Phys. Rev. D **79,** 064016 (2009).

[40] P. Pradhan, Stability analysis and quasinormal modes of Reissner–Nordstrøm space-time via Lyapunov exponent, Pramana **87,** 5 (2016).

[41] P. P. Pradhan, Lyapunov exponent and charged Myers Perry spacetimes, Eur. Phys. J. C **73,** 2477 (2013).

[42] K. Hashimoto, K. Murata, N. Tanahashi, and R. Watanabe, Bound on energy dependence of chaos, Phys. Rev. D **106,** 126010 (2022).

[43] K. Hashimoto and K. Sugiura, Causality bounds chaos in geodesic motions, Phys. Rev. D **107,** 066005 (2023).

[44] X. Guo, Y. Lu, B. Mu, and P. Wang, Probing phase structure of black holes with Lyapunov exponents, J. High Energy Phys. 08 (2022) 153.

[45] S. Jeong, B.-H. Lee, H. Lee, and W. Lee, Homoclinic orbit and the violation of chaos bound around the black hole with anisotropic matter fields, arXiv:2301.12198.